On a Geodesic Equation for Planar Conformal Template Matching

Stephen Marsland, Robert Mclachlan, Klas Modin, Matthew Perlmutter

On a Geodesic Equation for Planar Conformal Template Matching

Stephen Marsland[1], Robert McLachlan[2], Klas Modin[1], and Matthew Perlmutter[2]

[1] School of Engineering and Advanced Technology (SEAT)
Massey University, Palmerston North, New Zealand
[2] Institute of Fundamental Sciences (IFS)
Massey University, Palmerston North, New Zealand

Abstract. In this paper we consider planar conformal deformations, motivated by the warps that Wentworth Thompson used to deform images of one species into another. We study an equation for geodesic motion on the infinite dimensional Fréchet manifold $\mathrm{Con}(\mathbb{D}, \mathbb{R}^2)$ of conformal embeddings of the disk into the plane. We demonstrate that solutions may be represented as sheets, and use the sheet ansatz to derive a numerical discretization scheme. We also show that the equation admits totally geodesic solutions corresponding to scaling and translation, but not to affine transformations.

1 Introduction

The use of diffeomorphic transformations in both image registration and shape analysis is now common and utilised in many machine vision and image analysis tasks. One image or shape is brought into alignment with another by deforming the image until some similarity measure reaches a minimum. The deformation is computed as a geodesic with respect to some metric on the diffeomorphism group. For a general treatment and an overview of the subject see [1] and references therein.

The standard approach to the deformation method is to first perform an affine registration (principally to remove translation and rotation), and then to seek a diffeomorphic warp of the image. However, in what is arguably the most influential demonstration of the application of warping methods – D'Arcy Wentworth Thompson's seminal book 'On Growth and Form' [2] – Thompson transforms images of one species into another using relatively simple warps, so that the gross features of the two match. In a recent review of his work, biologist Arthur Wallace says:

This theory cries out for causal explanation, which is something the great man eschewed. [...] His transformations suggest coordinated rather than piecemeal changes to development in the course of evolution, an issue which almost completely disappeared from view in the era of the 'modern synthesis' of evolutionary theory, but which is of central importance again in the era of evo-devo.

[. . .] All the tools are now in place to examine the mechanistic basis of transformations. Not only do we have phylogenetic systematics and evo-devo, but, so obvious that it is easy to forget, we have computers, and especially, in this context, advanced computer graphics. We owe it to the great man to put these three things together to investigate the mechanisms that produce the morphological changes that he captured so elegantly with little more than sheets of graph paper and, of course, a brilliant mind. [3]

Figure no. in [2]	Transformation group
515	$x \mapsto ax,\ y \mapsto y$
513.2	$x \mapsto ax,\ y \mapsto by$
509, 510, 518	$x \mapsto ax,\ y \mapsto cx + dy$ (shears)
521–22, 513.5	$x \mapsto ax + by,\ y \mapsto cx + dy$ (affine)
506,508	$x \mapsto ax,\ y \mapsto g(y)$
511	$x \mapsto f(x),\ y \mapsto g(y)$
517–20, 523, 513.1, 513.3, 513.4, 513.6, 514, 525	conformal
524	'peculiar'

Table 1. Transformation groups used in some transformations in Chapter XII, 'On the Theory of Transformations, or the Comparison of Related Forms', of [2]

We draw attention to two key aspects of Thompson's examples: (i) the transformations are as simple as possible to achieve what he considers a good enough match (see Table 1); and (ii) the classes of transformations that he considers all forms groups (or pseudo groups), either finite or infinite dimensional. Mostly, he uses conformal transformations, a constraint he is reluctant to give up[3].

In terms of diffeomorphic image matching, Figs. 506, 508 and 511 of [2] are related to the one-dimensional diffeomorphism group, and hence to the Camassa–Holm family of equations [4]; but the groups usually studied in the literature are the full diffeomorphism group (two functions of two variables) and the volume-preserving group (one function of two variables). Conformal maps are defined by two functions of one variable: a drastically reduced dimensionality.

For applications in image registration we therefore suggest to vary the group from which warps are drawn as well as the metric. If a low-dimensional group gives a close match, then it should be preferred over a similar match from a higher-dimensional group; if necessary, local deformations from the full diffeo-

[3] "It is true that, in a mathematical sense, it is not a perfectly satisfactory or perfectly regular deformation, for the system is no longer isogonal; but[. . .] approaches to an isogonal system under certain conditions of friction or constraint." ([2], p. 1064) "[. . .] it will perhaps be noticed that the correspondence is not always quite accurate in small details. It could easily have been made much more accurate by giving a slightly sinuous curvature to certain of the coordinates. But as they stand, the correspondence indicated is very close, and the simplicity of the figures illustrates all the better the general character of the transformation." (ibid., p. 1074).

morphism group can be added later. In this paper we consider the case of conformal transformations.

Although the composition of two conformal maps $\mathbb{R}^2 \to \mathbb{R}^2$ is conformal, it need not be invertible: we need to restrict the domain. The invertible conformal maps $\mathbb{D} \to \mathbb{D}$ do form a group, the disk-preserving Möbius group, but it is only 3 dimensional. We are therefore led to consider the infinite dimensional configuration space $\mathrm{Con}(\mathbb{D}, \mathbb{R}^2)$ of planar conformal embeddings of the closed unit disk $\mathbb{D}$ into the plane. This is not a group, but it is a pseudo group.

2 Derivation of the Weak Geodesic Equation

In this section we give a derivation of the weak form of the governing equation.

Let g denote the Euclidean metric on $\mathbb{R}^2$, i.e., in Cartesian coordinates we have $\mathsf{g} = \mathrm{d}x \otimes \mathrm{d}x + \mathrm{d}y \otimes \mathrm{d}y$. Then $(\mathbb{D}, \mathsf{g})$ is a compact Riemannian manifold with boundary. The linear space $C^\infty(\mathbb{D}, \mathbb{R}^2)$ of smooth maps $\mathbb{D} \to \mathbb{R}^2$ is a Fréchet space (see [5, Sect. I.1] for details on the Fréchet topology used). The set $\mathrm{Emb}(\mathbb{D}, \mathbb{R}^2)$ of smooth embeddings of the disk into the plane is an open subset of $C^\infty(\mathbb{D}, \mathbb{R}^2)$ and has the structure of a Fréchet manifold (see [5, Sect. I.4.1]). The subspace $C^\infty_{\mathrm{c}}(\mathbb{D}, \mathbb{R}^2) = \{\phi \in C^\infty(\mathbb{D}, \mathbb{R}^2); \phi^* \mathsf{g} = F\mathsf{g}, F \in \mathcal{F}(\mathbb{D})\}$ of maps preserving the metric up to a scalar function is topologically closed in $C^\infty(\mathbb{D}, \mathbb{R}^2)$. Furthermore, it holds that the set of conformal embeddings $\mathrm{Con}(\mathbb{D}, \mathbb{R}^2) = C^\infty_{\mathrm{c}}(\mathbb{D}, \mathbb{R}^2) \cap \mathrm{Emb}(\mathbb{D}, \mathbb{R}^2)$ is a Fréchet submanifold of $\mathrm{Emb}(\mathbb{D}, \mathbb{R}^2)$.

For standard planar template matching equations, one introduces a positive-definite quadratic Lagrangian function (corresponding to a weak Riemannian structure) on the infinite dimensional manifold $\mathrm{Diff}(\mathbb{D}) = \mathrm{Emb}(\mathbb{D}, \mathbb{D})$. However, as mentioned above, the set $\mathrm{Diff}_{\mathrm{c}}(\mathbb{D})$ of disk preserving conformal maps is small, so we consider instead $\mathrm{Con}(\mathbb{D}, \mathbb{R}^2)$ as configuration manifold. The Riemann mapping theorem asserts that $\mathrm{Con}(\mathbb{D}, \mathbb{R}^2)$ contains a rich set of maps: for any simply connected domain $\mathsf{U} \subset \mathbb{R}^2$ we can find $\varphi \in \mathrm{Con}(\mathbb{D}, \mathbb{R}^2)$ such that $\varphi(\mathbb{D}) = \mathsf{U}$, and φ is then unique up to the disk-preserving Möbius transformations. That is, φ must be an element of a unique co-set $[\varphi] \in \mathrm{Con}(\mathbb{D}, \mathbb{R}^2)/\mathrm{Diff}_{\mathrm{c}}(\mathbb{D})$, where $\mathrm{Diff}_{\mathrm{c}}(\mathbb{D})$ acts on $\mathrm{Con}(\mathbb{D}, \mathbb{R}^2)$ by composition from the right. Thus, it holds that $\mathrm{Con}(\mathbb{D}, \mathbb{R}^2)/\mathrm{Diff}_{\mathrm{c}}(\mathbb{D})$ is equivalent to the well known *shape space* $\mathrm{Emb}(\mathbb{D}, \mathbb{R}^2)/\mathrm{Diff}(\mathbb{D})$, so we expect that the equation studied in this paper will be relevant not only for conformal image matching, but also for planar shape matching[4]. Also, as developed in [6], a planar shape may, by conformal mappings, be represented by a *fingerprint* in $\mathrm{Diff}(S^1)$, which suggests that $\mathrm{Diff}(S^1)$ may be used for co-sets.

Since $\mathrm{Con}(\mathbb{D}, \mathbb{R}^2)$ is open in the linear space $C^\infty_{\mathrm{c}}(\mathbb{D}, \mathbb{R}^2)$ its tangent bundle is $T\mathrm{Con}(\mathbb{D}, \mathbb{R}^2) = \mathrm{Con}(\mathbb{D}, \mathbb{R}^2) \times C^\infty_{\mathrm{c}}(\mathbb{D}, \mathbb{R}^2)$. The Lagrangian we are interested in is given by

$$L(\varphi, \dot{\varphi}) = \frac{1}{2} \int_{\varphi(\mathbb{D})} \mathsf{g}(\dot{\varphi} \circ \varphi^{-1}, \dot{\varphi} \circ \varphi^{-1}) \, \mathrm{d}A \tag{1}$$

[4] This is only true in $\mathbb{R}^2$: for higher dimensions the set of conformal embeddings of the unit ball $\mathcal{B}$ is very small, and it does not hold that $\mathrm{Con}(\mathcal{B}, \mathbb{R}^n)/\mathrm{Diff}_{\mathrm{c}}(\mathcal{B})$ and $\mathrm{Emb}(\mathcal{B}, \mathbb{R}^n)/\mathrm{Diff}(\mathcal{B})$ are equivalent.

where $\mathrm{d}A = \mathrm{d}x \wedge \mathrm{d}y$ is the standard Euclidean area form on $\mathbb{R}^2$ associated with g.

Note that φ^{-1} is well-defined as a map $\varphi(\mathbb{D}) \to \mathbb{D}$ and that the Lagrangian is well-defined on the full embedding manifold $\mathrm{Emb}(\mathbb{D}, \mathbb{R}^2)$. It is quadratic in $\dot{\varphi}$ and positive-definite, thus determining a (weak) Riemannian metric. When restricted to the submanifold $\mathrm{Diff}(\mathbb{D})$ of $\mathrm{Emb}(\mathbb{D}, \mathbb{R}^2)$, this metric coincides with the metric used in the L^2 template matching equation (TME). Further, $\mathrm{Diff}_\mathrm{c}(\mathbb{D})$ is a right symmetry group: if $\phi \in \mathrm{Diff}_\mathrm{c}(\mathbb{D})$ then $L(\varphi \circ \phi, \dot{\varphi} \circ \phi) = L(\varphi, \dot{\varphi})$. In turn, this implies that we obtain a *reduced variational principle* with respect to the reduced variable $\xi = \dot{\varphi} \circ \varphi^{-1} \in \mathfrak{X}_\mathrm{c}(\varphi(\mathbb{D}))$, where $\mathfrak{X}_\mathrm{c}(\varphi(\mathbb{D}))$ denotes the set of conformal vector fields (whose flow is conformal). However, we still need to keep track of the correct domain $\varphi(\mathbb{D})$, which corresponds to the "shape space" element in $\mathrm{Con}(\mathbb{D}, \mathbb{R}^2)/\mathrm{Diff}_\mathrm{c}(\mathbb{D})$, so the complete set of reduced variables consists of a domain $\mathsf{U} \in \mathcal{R}(\mathbb{R}^2)$ (where $\mathcal{R}(\mathbb{R}^2)$ is the Fréchet manifold of simply connected compact planar regions, see [5, Sect. I.4.3]), and a conformal vector field $\xi \in \mathfrak{X}_\mathrm{c}(\mathsf{U})$ defined on this domain. Thus, the reduced phase space is the Fréchet tangent bundle $\mathfrak{X}(\mathcal{R}(\mathbb{R}^2))$ over $\mathcal{R}(\mathbb{R}^2)$, such that the fibre over U is the vector space $\mathfrak{X}_\mathrm{c}(\mathsf{U})$ of conformal vector fields (see [7] for details). For $\xi, \eta \in \mathfrak{X}(\mathsf{U})$ let $\langle \xi, \eta \rangle_\mathsf{U} := \int_\mathsf{U} \mathsf{g}(\xi, \eta) \mathrm{d}A$. The variational principle then becomes

$$0 = \frac{\mathrm{d}}{\mathrm{d}\varepsilon}\Big|_{\varepsilon=0} \int_0^1 L(\varphi_\varepsilon, \dot{\varphi}_\varepsilon)\, \mathrm{d}t = \frac{\mathrm{d}}{\mathrm{d}\varepsilon}\Big|_{\varepsilon=0} \int_0^1 \frac{1}{2} \langle \xi_\varepsilon, \xi_\varepsilon \rangle_{\mathsf{U}_\varepsilon}\, \mathrm{d}t \tag{2}$$

where φ_ε is a variation of an extremal curve $t \mapsto \varphi(t)$ in $\mathrm{Con}(\mathbb{D}, \mathbb{R}^2)$ and

$$(\mathsf{U}_\varepsilon, \xi_\varepsilon) := (\varphi_\varepsilon(\mathbb{D}), \dot{\varphi}_\varepsilon \circ \varphi_\varepsilon^{-1}).$$

Since a general variation of $t \to \varphi(t)$ is of the form $\exp(\varepsilon\eta) \circ \varphi$ (where $t \mapsto \eta(t)$ is a path in $\mathfrak{X}_\mathrm{c}(\varphi(\mathbb{D}))$ with vanishing endpoints) direct calculation yields

$$\begin{aligned} \frac{\mathrm{d}}{\mathrm{d}\varepsilon}\Big|_{\varepsilon=0} \xi_\varepsilon &= \dot{\eta} + \pounds_\eta \xi \\ \frac{1}{2}\frac{\mathrm{d}}{\mathrm{d}\varepsilon}\Big|_{\varepsilon=0} \langle \xi, \xi \rangle_{\mathsf{U}_\varepsilon} &= \langle \pounds_\eta \xi, \xi \rangle_\mathsf{U} + \int_\mathsf{U} \mathsf{g}(\xi, \xi)\, \mathrm{div}(\eta) \mathrm{vol}. \end{aligned}$$

where $\pounds_\eta$ denotes the Lie derivative along η. Plugging this into (2) yields the weak form of a planar conformal template matching equation (PCTME) to be studied in this paper:

$$\int_0^1 \langle \xi, \dot{\eta} + 2\pounds_\eta \xi + \mathrm{div}(\eta)\xi \rangle_\mathsf{U}\, \mathrm{d}t = 0 \tag{3}$$

for all variations $t \mapsto \eta(t) \in \mathfrak{X}(\mathsf{U}(t))$, where $t \mapsto \mathsf{U}(t)$ fulfills the "compatibility" equation $\dot{\mathsf{U}} = \xi(\partial\mathsf{U})$ and $\mathsf{U}(0) = \mathbb{D}$, i.e., the domain is transported along the flow generated by ξ. In practice, however, we do not solve for the domain variable U, but instead we immediately solve the reconstruction equation $\dot{\varphi} = \xi \circ \varphi$, and use the fact that $\mathsf{U} = \varphi(\mathbb{D})$.

2.1 The Complex Form

By identifying $\mathbb{R}^2$ with $\mathbb{C}$ the space $\mathfrak{X}_c(\mathsf{U})$ is identified with the space of holomorphic functions in the complex domain $\mathsf{U} \subset \mathbb{C}$. Likewise, $C_c^\infty(\mathbb{D}, \mathbb{R}^2)$ is identified with the space of holomorphic function on $\mathbb{D} \subset \mathbb{C}$, and $\mathrm{Con}(\mathbb{D}, \mathbb{R}^2)$ with the space of injective holomorphic functions on $\mathbb{D}$. We therefore identify $\varphi, \dot{\varphi}$ as holomorphic functions on $\mathbb{D}$, and φ^{-1}, ξ as holomorphic functions on $\varphi(\mathbb{D})$. The complex derivative of a holomorphic function is denoted by a prime, e.g., ξ' for $z \mapsto \xi'(z)$.

When working with complex entries, it is useful to express the weak form (3) in terms of the Hermitian inner product $\langle\!\langle \xi, \eta \rangle\!\rangle_{\mathsf{U}} = \int_{\mathsf{U}} \xi \overline{\eta} \, \mathrm{d}A$ instead of the real-valued inner product.

Direct calculation yields that $\mathsf{g}(\xi, \mathrm{div}(\eta)\xi) + \mathrm{i}\mathsf{g}(\xi, \mathrm{div}(\mathrm{i}\eta)\xi) = 2\xi\overline{\eta'\xi}$. Using this and the fact that $\langle\!\langle \xi, \eta \rangle\!\rangle_{\varphi(\mathbb{D})} = \langle \xi, \eta \rangle_{\varphi(\mathbb{D})} + \mathrm{i}\langle \xi, \mathrm{i}\eta \rangle_{\varphi(\mathbb{D})}$ we obtain the complex weak form of the PCTME (3) as (where we write $\varphi(\mathbb{D})$ instead of U to indicate that we choose to simultaneously solve the reconstruction equation $\dot{\varphi} = \xi \circ \varphi$, instead of only solving for U)

$$\int_0^1 \langle\!\langle \xi, \dot{\eta} + 4\eta'\xi - 2\xi'\eta \rangle\!\rangle_{\varphi(\mathbb{D})} \, \mathrm{d}t = 0. \tag{4}$$

We investigate a sheet ansatz for this equation in Section 4, leading to a numerical discretization, but first we consider a set of special solutions to this equation, by identifying a totally geodesic submanifold of $\mathrm{Con}(\mathbb{D}, \mathbb{R}^2)$.

3 Totally Geodesic Submanifolds

Recall that a submanifold $N \subset M$ of a Riemannian manifold (M, g) is *totally geodesic with respect to* (M, g) if geodesics in N (with respect to g restricted to N) are also geodesics in M. For a thorough treatment of totally geodesic subgroups of $\mathrm{Diff}(M)$ (with respect to various metrics), see [8].

Consider the Fréchet submanifold of linear conformal transformations

$$\mathrm{Lin}(\mathbb{D}, \mathbb{R}^2) = \left\{ \varphi \in \mathrm{Con}(\mathbb{D}, \mathbb{R}^2); \varphi(z) = cz, c \in \mathbb{C} \right\}.$$

Proposition 1. $\mathrm{Lin}(\mathbb{D}, \mathbb{C})$ *is totally geodesic in* $\mathrm{Con}(\mathbb{D}, \mathbb{C})$.

Proof. If $t \mapsto \varphi(t)$ is a path in $\mathrm{Lin}(\mathbb{D}, \mathbb{C})$, i.e., $\varphi(z) = cz$ with $c \in \mathbb{C}$, then $\xi = \dot{\varphi} \circ \varphi^{-1}$ is of the form $\xi(z) = az$ with $a \in \mathbb{C}$. Now, let $t \mapsto (\varphi, \xi)$ fulfill the variational equation (4) for each variation of the form $\eta(z) = bz$ with $b \in \mathbb{C}$. We need to show that $t \mapsto (\varphi, \xi)$ then fulfills the equation for any variation of the form $\eta(z) = ez^k$ (since the monomials span the space of holomorphic functions). Thus,

$$\begin{aligned} \langle\!\langle \xi, \dot{\eta} + 4\eta'\xi - 2\xi'\eta \rangle\!\rangle_{\varphi(\mathbb{D})} &= \langle\!\langle \varphi' \cdot \xi \circ \varphi), \varphi' \cdot (\dot{\eta} + 4\eta'\xi - 2\xi'\eta) \circ \varphi \rangle\!\rangle_{\mathbb{D}} \\ &= |c|^4 \langle\!\langle az, \dot{b}z^k + 4kbaz^k - 2abz^k \rangle\!\rangle_{\mathbb{D}}. \end{aligned} \tag{5}$$

where in the first line we use the conformal change of variables formula for integrals. Now, since the monomials are orthogonal with respect to $\langle\!\langle \cdot, \cdot \rangle\!\rangle_{\mathbb{D}}$ the expression vanish whenever $k \neq 1$, which concludes the proof. □

From equation (5) we may derive a differential equation for the totally geodesic solutions in $\mathrm{Lin}(\mathbb{D},\mathbb{C})$ in term of the variables (c,a) corresponding to $\varphi(z)=cz$ and $\xi(z)=az$. Indeed, choosing $k=1$ and plugging equation (5) into the variational equation (4) we obtain

$$\begin{aligned}0&=\int_0^1 |c|^4(a\dot{\bar{b}}+2|a|^2\bar{b})\,\mathrm{d}t=\int_0^1\Big(\frac{\mathrm{d}}{\mathrm{d}t}a\bar{b}|c|^4-\bar{b}\big(\frac{\mathrm{d}}{\mathrm{d}t}a|c|^4-2|a|^2|c|^4\big)\Big)\,\mathrm{d}t\\&=-\int_0^1\bar{b}\big(\dot{a}|c|^4+2a\dot{c}\bar{c}|c|^2+2a\dot{\bar{c}}c|c|^2-2|a|^2|c|^4\big)\\&=-\int_0^1\bar{b}|c|^4\big(\dot{a}+2a\big)\end{aligned}$$

where we have used that b vanish at the endpoints, and in the last line we use that $\dot{c}=ac$, which follows since $\dot{\varphi}=\xi\circ\varphi$. Hence, the governing equations for the totally geodesic solutions are

$$\begin{aligned}\dot{c}&=ac\\\dot{a}&=-2a^2\end{aligned}\tag{6}$$

where $c(0)=1$ (since $\varphi(z)=z$ initially). We can see that if $a(0)$ is real, then both a and c stay real, so that the smaller submanifold of pure scalings is also totally geodesic. However, pure rotations are *not* totally geodesic.

By using again the weak form (4) of the governing equation one can further show that the submanifold of translations is *not* totally geodesic in $\mathrm{Con}(\mathbb{D},\mathbb{C})$. Nor is the submanifold of affine conformal transformations. The result is somewhat surprising, given that these types of basic transformations are totally geodesic for the L^2–TME and H^1_α–TME[5], if boundary conditions are set up to allow them [8]. In fact, from a template matching point of view, where basic transformations should preferably be totally geodesic, our result indicates that the metric we have picked is not ideal.

4 Sheet Ansatz

The L^2–TME and H^1_α–TME are known to admit solutions corresponding to totally geodesic submanifolds described by momentum particles or sheets [9]. These special solutions can be used for structure preserving numerical discretization [10,11]. Since the ansatz is non-smooth (the momentum is a traveling peakon), it cannot describe solutions to the conformal equation studied here. However, in this section we show that it is possible to express solutions to the PCTME (4) with a different sheet ansatz, using a reproducing kernel.

Let $\mathcal{O}\subset\mathbb{C}$ be an open bounded complex region. Then $A^2(\mathcal{O})=\{f\in L^2(\mathcal{O});\, f \text{ is holomorphic}\}$ is a Hilbert space with the inner product $\langle\!\langle\cdot,\cdot\rangle\!\rangle_{\mathcal{O}}$ (called

[5] Also called the *EPDiff equation* or the *averaged template matching equation*.

a *Bergman space*, see [12, Ch. 1]). For any $z \in \mathcal{O}$ it holds that point-wise evaluation $E_z : \xi \mapsto \xi(z)$ is continuous with respect to $\langle\!\langle \cdot, \cdot \rangle\!\rangle_{\mathcal{O}}$. Thus, by the Riesz representation theorem there exists a unique $k_z \in A^2(\mathcal{O})$ such that $f(z) = \langle\!\langle f, k_z \rangle\!\rangle_{\mathcal{O}}$ for every $f \in A^2(\mathcal{O})$. Let $\mathsf{U} = \overline{\mathcal{O}}$ be the closure of $\mathcal{O}$. Since $\mathfrak{X}_{\mathrm{c}}(\mathsf{U}) \subset A^2(\mathcal{O})$ it clearly holds that $\xi(z) = \langle\!\langle \xi, k_z \rangle\!\rangle_{\mathsf{U}}$ for all $\xi \in \mathfrak{X}_{\mathrm{c}}(\mathsf{U})$ (however, notice that it does *not* hold that $k_z \in \mathfrak{X}_{\mathrm{c}}(\mathsf{U})$). The function defined by $K_{\mathsf{U}}(z, w) = \overline{k_z(w)}$ is called the *reproducing kernel* (or sometimes the *Bergman kernel function*) for the domain U. On the interior of U this function is analytic in z and anti-analytic in w, with $K(z, w) = \overline{K(w, z)}$. Furthermore, if $\varphi \in \mathrm{Con}(\mathbb{D}, \mathbb{C})$, then

$$K_{\varphi(\mathbb{D})}(z, w) = \frac{K_{\mathbb{D}}(\varphi^{-1}(z), \varphi^{-1}(w))}{\varphi'(\varphi^{-1}(z))\overline{\varphi'(\varphi^{-1}(w))}} \tag{7}$$

which follows by a change of variables in the integral over $\varphi(\mathbb{D})$. When working with kernels in practice, e.g., for numerical purposes, this formula is very useful since the kernel function for the disk is known to be

$$K_{\mathbb{D}}(z, w) = \frac{1}{\pi} \frac{1}{(1 - z\overline{w})^2} \quad .$$

Now, consider the following ansatz:

$$\xi(z) = \int_0^{2\pi} p_\varphi(\rho \mathrm{e}^{\mathrm{i}s}) K_{\varphi(\mathbb{D})}\big(z, \varphi(\rho \mathrm{e}^{\mathrm{i}s})\big) \mathrm{d}s \tag{8}$$

where $p_\varphi \in C_{\mathrm{c}}^\infty(\mathbb{D}, \mathbb{C})$ and $0 < \rho < 1$ is a fixed constant. We introduce the periodic functions $\gamma, p_\gamma : S^1 \to \mathbb{C}$ defined by $\gamma(s) = \varphi(\rho \mathrm{e}^{\mathrm{i}s})$ and $p_\gamma(s) = p_\varphi(\rho \mathrm{e}^{\mathrm{i}s})$, so that $\xi(z) = \int_0^{2\pi} p_\gamma K_{\varphi(\mathbb{D})}(z, \gamma) \mathrm{d}s$. One may think of $\gamma(s)$ as just a notational shortcut, but it has other significance: by expanding φ as a Taylor series with coefficients $(c_k)_{k=0}^\infty$, we see that the periodic curve $\gamma(s)$ only has positive Fourier coefficients, which are given by $(\rho^k c_k)_{k=0}^\infty$. An equivalent statement is to say that the Fourier coefficients of $\gamma(s)$ are the Taylor coefficients of $z \mapsto \varphi(\rho z)$. Exactly the same relation holds between p_γ and p_φ. This observation can be used in the numerical discretization to accelerate the evaluation of the right-hand side using fast Fourier transformations.

Plugging the ansatz (8) into the weak equation (4) yields

$$\begin{aligned}
0 &= \int_0^1 \int_0^{2\pi} \overline{p_\gamma} \langle\!\langle \dot{\eta} + 4\eta'\xi - 2\xi'\eta, K_{\varphi(\mathbb{D})}(\cdot, \gamma) \rangle\!\rangle_{\varphi(\mathbb{D})} \, \mathrm{d}s \, \mathrm{d}t \\
&= \int_0^1 \int_0^{2\pi} \overline{p_\gamma} \Big(\dot{\eta}(\gamma) + 4\eta'(\gamma)\xi(\gamma) - 2\xi'(\gamma)\eta(\gamma) \Big) \, \mathrm{d}s \, \mathrm{d}t \\
&= \int_0^1 \int_0^{2\pi} \Big(\eta(\gamma) \Big(-\overline{\dot{p}_\gamma} - 2\overline{p_\gamma}\xi'(\gamma) \Big) + \overline{p_\gamma}\eta'(\gamma) \Big(4\xi(\gamma) - \dot{\gamma} \Big) \Big) \, \mathrm{d}s \, \mathrm{d}t
\end{aligned}$$

where we use the evaluation property of the kernel in the second line and the fact that $t \mapsto \eta(t)$ vanish at the endpoints in the third. Next, using that $\dot{\gamma}(s) =$

$\dot{\varphi}(\rho e^{is}) = \xi(\varphi(\rho e^{is})) = \xi(\gamma(s))$, we get

$$\begin{aligned} 0 &= \int_0^1 \int_0^{2\pi} \left(\eta(\gamma) \Big(-\overline{\dot{p}_\gamma} - 2\overline{p_\gamma}\xi'(\gamma) \Big) + \overline{p_\gamma}\eta'(\gamma)\, 3\xi(\gamma) \right) \mathrm{d}s\, \mathrm{d}t \\ &= \int_0^1 \int_0^{2\pi} \left(\eta(\gamma) \Big(-\overline{\dot{p}_\gamma} - 2\overline{p_\gamma}\xi'(\gamma) \Big) + \eta'(\gamma)\gamma' \left(\frac{3\overline{p_\gamma}\xi(\gamma)}{\gamma'} \right) \right) \mathrm{d}s\, \mathrm{d}t \\ &= \int_0^1 \int_0^{2\pi} \left(\eta(\gamma) \left(-\overline{\dot{p}_\gamma} - 2\overline{p_\gamma}\xi'(\gamma) \right) - \eta(\gamma) \frac{\partial}{\partial s} \left(\frac{3\overline{p_\gamma}\xi(\gamma)}{\gamma'} \right) \right) \mathrm{d}s\, \mathrm{d}t \\ &= -\int_0^1 \int_0^{2\pi} \eta(\gamma) \left(\overline{\dot{p}_\gamma} - 2\xi(\gamma) \frac{\partial}{\partial s} \left(\frac{\overline{p_\gamma}}{\gamma'} \right) + 5 \frac{\partial}{\partial s} \left(\frac{\overline{p_\gamma}\xi(\gamma)}{\gamma'} \right) \right) \mathrm{d}s\, \mathrm{d}t \end{aligned} \tag{9}$$

where γ' denotes the derivative of γ with respect to s. Thus, by inserting the ansatz (8) we obtain a weak formulation of the PCTME, equivalent to (4), in terms of the variables γ and p_γ. This form involves an integral operator, since ξ is related to γ, p_γ by the ansatz (8).

In contrast to the L^2–TME and H^1_α–TME, *any* solution to the PCTME can be represented by the sheet ansatz, since any φ can be reconstructed from γ by the Fourier transformation.

A nice feature of the weak formulation (9) is that the test function η is isolated, i.e., without derivatives. This allows us to use the fundamental lemma of calculus of variations to get rid of the outermost time integral (so we get a condition at each fixed point in time). However, we do not immediately obtain a strong formulation, because the test function η must be holomorphic, so we cannot use the fundamental lemma of calculus of variations for the inner integral without introducing a projection operator. Since the trigonometric monomials e^{iks} are orthogonal with respect to the s–integral, the projection is given by neglecting negative Fourier coefficients. Hence, let $\chi_+ : \mathbb{Z} \to \mathbb{R}$ be the sequence

$$\chi_+(k) = \begin{cases} 1 \text{ if } k \geq 0 \\ 0 \text{ if } k < 0 \end{cases}$$

and let $\mathcal{F}$ denote the Fourier operator taking a 2π–periodic function to its Fourier series. Then the projection operator is given by $\mathcal{P} = \mathcal{F}^{-1}\chi_+\mathcal{F}$ (where χ_+ is acing by element-wise multiplication). We now obtain a strong integral formulation of the PCTME in terms of γ and p_γ as

$$\begin{aligned} \dot{\gamma} &= \xi(\gamma) \\ \dot{p}_\gamma &= \mathcal{P}\left(2\overline{\xi(\gamma)} \frac{\partial}{\partial s} \frac{p_\gamma}{\overline{\gamma'}} - 5 \frac{\partial}{\partial s} \frac{p_\gamma \overline{\xi(\gamma)}}{\overline{\gamma'}} \right) . \end{aligned} \tag{10}$$

5 Numerical Discretization

In this section we describe a method for numerical discretization of equations (10). The idea is to represent the dynamic variables $\gamma(s)$ and $p_\gamma(s)$ by truncated positive Fourier series, or, equivalently, truncated Taylor series of $z \mapsto \varphi(\rho z)$ and

$z \mapsto p_\varphi(\rho z)$. Thus, our finite set of dynamic variables are $\boldsymbol{c} = (c_k)_{k=0}^{n-1} \in \mathbb{C}^n$ and $\boldsymbol{p_c} = (p_k)_{k=0}^{n-1} \in \mathbb{C}^n$ such that

$$\gamma(s) = \varphi(\rho \mathrm{e}^{\mathrm{i}s}) = \sum_{k=0}^{n-1} c_k \mathrm{e}^{\mathrm{i}s}, \quad p_\gamma(s) = p_\varphi(\rho \mathrm{e}^{\mathrm{i}s}) = \sum_{k=0}^{n-1} p_k \mathrm{e}^{\mathrm{i}s}. \tag{11}$$

For the discretization we insert these into the right-hand side of equation (10) and compute the first n positive Fourier coefficients, which then gives an ordinary differential equation for $(\boldsymbol{c}, \boldsymbol{p_c}) \in \mathbb{C}^{2n}$. We now describe how this discretized right-hand side is computed efficiently.

1. Compute $\boldsymbol{\gamma} = (\gamma(0), \gamma(\pi/n), \dots, \gamma(\pi(2n-1)/n))$ from $\boldsymbol{c}$. (Notice that $\boldsymbol{\gamma}$ has length $2n$.) Since $\gamma(s) = \varphi(\rho \mathrm{e}^{\mathrm{i}s})$ and $\boldsymbol{c}$ are the Taylor coefficients of $z \mapsto \varphi(\rho z)$, we obtain $\boldsymbol{\gamma}$ from the inverse FFT as $\boldsymbol{\gamma} = 2n\,\mathrm{IFFT}(\boldsymbol{c}^+)$, where $\boldsymbol{c}^+ = (\boldsymbol{c}, 0, \dots, 0)$ is zero-padded to get the same length as $\boldsymbol{\gamma}$ (since in the FFT the last half of the vector corresponds to negative frequencies).
2. Compute $\boldsymbol{p_\gamma} = (p_\gamma(0), \dots, p_\gamma(\pi(2n-1)/n))$ from $\boldsymbol{p_c}$. By the same argument we have $\boldsymbol{p_\gamma} = 2n\,\mathrm{IFFT}(\boldsymbol{p_c})$.
3. Compute $\boldsymbol{\gamma}' = (\gamma'(0), \gamma'(2\pi/n), \dots, \gamma'(2\pi(n-1)/n))$. Since the Fourier coefficients of $\gamma(s)$ are given by $\boldsymbol{c}$, we have $\boldsymbol{\gamma}' = 2n\,\mathrm{IFFT}(\mathrm{i}\boldsymbol{k}^+ \cdot \boldsymbol{c}^+)$ where $\boldsymbol{k} = (0, 1, \dots, n-1)$ and $\boldsymbol{k}^+ \cdot \boldsymbol{c}^+$ denotes element-wise multiplication.
4. Compute $\boldsymbol{\xi} = (\xi(\boldsymbol{\gamma}_0), \dots, \xi(\boldsymbol{\gamma}_{2n-1}))$. From the ansatz (8) and the equation for the Bergman kernel (7), we get

$$\xi(\gamma(s)) = \int_0^{2\pi} \frac{p_\gamma(\sigma) K_{\mathbb{D}}(\rho \mathrm{e}^{\mathrm{i}s}, \rho \mathrm{e}^{\mathrm{i}\sigma})}{\varphi'(\rho \mathrm{e}^{\mathrm{i}s}) \overline{\varphi'(\rho \mathrm{e}^{\mathrm{i}\sigma})}} \mathrm{d}\sigma = \frac{1}{\pi \gamma'(s)} \int_0^{2\pi} \frac{p_\gamma(\sigma) G(\rho^2 \mathrm{e}^{\mathrm{i}(s-\sigma)})}{\overline{\gamma'(\sigma)}}$$

   where $G(z) = z/(1-z)^2$. Now, set $f(s) = p_\gamma(s)/\overline{\gamma'(s)}$ and $g(s) = G(\rho^2 \mathrm{e}^{\mathrm{i}s})$. Then

$$\xi(\gamma(s)) = \frac{1}{\pi \gamma'(s)} \int_0^{2\pi} f(\sigma) g(s-\sigma) \mathrm{d}\sigma = \frac{(f * g)(s)}{\pi \gamma'(s)}.$$

   Thus, using that a convolution becomes element-wise multiplication in the Fourier domain, we get $\boldsymbol{\xi} = \frac{2n}{\pi}\,\mathrm{IFFT}(\hat{\boldsymbol{f}} \cdot \hat{\boldsymbol{g}})/\boldsymbol{\gamma}'$ where $\hat{\boldsymbol{g}} = (0, \rho^2, \dots, \rho^{2(n-1)}(n-1), 0, \dots, 0)$, which follows by computing the Taylor coefficients of $G(z)$, and $\hat{\boldsymbol{f}} = \mathrm{FFT}(\boldsymbol{p_\gamma}/\overline{\boldsymbol{\gamma}'})/2n$ (divisions are carried out element-wise).
5. Compute $\dot{\boldsymbol{c}}$. Using again the correspondence between Taylor and Fourier coefficients, we get $\dot{\boldsymbol{c}} = \mathrm{FFT}(\boldsymbol{\xi})^-/2n$, where the $\mathrm{FFT}(\boldsymbol{\xi})^-$ means that we only keep the first n elements. Thus, we have now computed the first half of the right-hand side.
6. Compute $\dot{\boldsymbol{p}}_{\boldsymbol{c}}$. From the second equation in (10) we get

$$\dot{\boldsymbol{p}}_{\boldsymbol{c}} = \mathrm{FFT}(2\overline{\boldsymbol{\xi}} \cdot \mathrm{IFFT}(\mathrm{i}\boldsymbol{k}^+ \cdot \hat{\boldsymbol{f}}))^- - 5\mathrm{i}\boldsymbol{k} \cdot \mathrm{FFT}(\overline{\boldsymbol{\xi}} \cdot \boldsymbol{p_\gamma}/\overline{\boldsymbol{\gamma}'})^-/2n.$$

   Note that the projection (corresponding to the operator $\mathcal{P}$ in equation (10)) occurs in the above computation since we only keep elements corresponding to positive frequencies.

We have now computed the full right-hand side $(\dot{\boldsymbol{c}}, \dot{\boldsymbol{p}}_{\boldsymbol{c}})$. By using a time-stepping method for ODEs (e.g., a Runge-Kutta method), a numerical method for equation (10) is obtained. Each evaluation of the right-hand side requires element-wise operations and 9 FFTs on vectors of length $2n$, which leads to complexity $\mathcal{O}(n \log(2n))$.

6 Experimental Results

In this section we study the dynamical behaviour of some solutions to the PCTME. First, we look at the solutions corresponding to the totally geodesic submanifold derived in Section 3. Thereafter, we use the numerical method derived in Section 5 to study other solutions. In particular, we study the spectrum of small perturbations of a totally geodesic solution.

6.1 Totally Geodesic Solutions

Let $\varphi_0(z) = z$ be the identity maps, and let $\varphi_1(z) = c_1 z$ where $c_1 \in \mathbb{C}\backslash\{0\}$. Since both φ_0 and φ_1 belong to the totally geodesic submanifold $\mathrm{Lin}(\mathbb{D}, \mathbb{C})$, the geodesic from φ_0 to φ_1 stays in $\mathrm{Lin}(\mathbb{D}, \mathbb{C})$. In Fig. 1 the geodesics for $c_1 = 0.2$ (scaling of the disk) and $c_1 = \mathrm{e}^{1.6\pi\mathrm{i}}$ (rotation of the disk) are shown. The solutions confirm what we earlier noticed, that pure scalings are totally geodesic (the curve $\varphi(t)$ remains a scaling for each t) whereas the geodesic corresponding to the rotated disk does not stay a pure rotation, but contains scaling along its path.

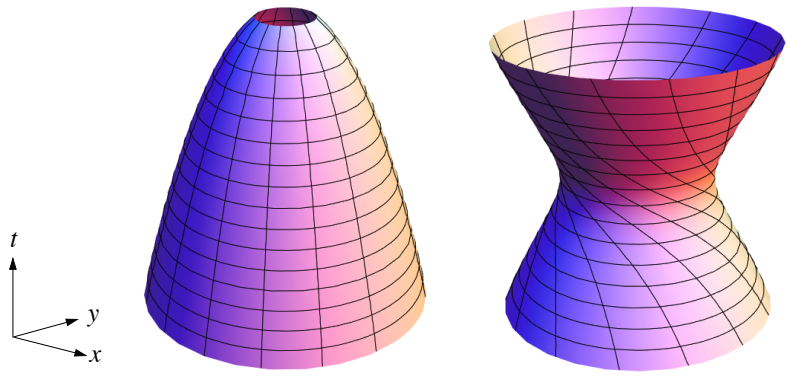

Fig. 1. Geodesic curve from $\varphi_0(z) = z$ to $\varphi_1(z) = c_1 z$ for different values of c_0. The mesh lines show how the unit circle evolves. Notice that the scaling geodesic stays a scaling (left figure), whereas the rotation geodesic picks up some scaling during its time evolution (right figure).

6.2 Development of Cusps in Finite Time

The L^2–TME is known to develop singularities in finite time. Originally, we expected solutions to the PCTME be more "well behaved" due to the holomorphic constraint. However, experiments with the numerical method derived in Section 5 indicates that the same phenomenon still occurs despite of the constraint. For example, Fig. 2 shows an experiment with initial data of the form $\dot{\varphi}_0(z) = a_2 z^2$. A cusp develops in the solution, which leads to a breakdown of the dynamics.

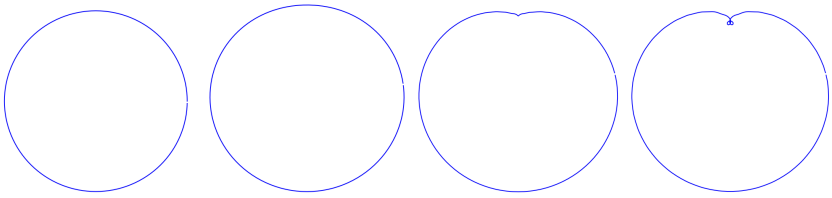

Fig. 2. Time evolution of the PCTME with initial conditions of the form $\varphi_0(z) = z$ and $\dot{\varphi}_0(z) = a_2 z^2$. From left to right the plots show the development of a cusp. Thus, the geodesic curve ceases to exist in finite time.

6.3 Spectral Behaviour

In Fig. 3 the time evolution of the absolute values of $\boldsymbol{p_c}$, computed with the numerical method in Section 5, are shown in two plots. Dark colours corresponds to low order coefficients, and light colours to high order coefficients. In the top plot, initial data corresponding to a totally geodesic solution in $\mathrm{Lin}(\mathbb{D}, \mathbb{C})$ are used. In the bottom plot, this initial data is perturbed $\dot{\varphi}_0(z) = a_1 z + \delta(z)$, where $\delta(z)$ is a small perturbation of the first five Taylor coefficients.

Notice in both plots that the initially suppressed coefficients grow exponentially fast, which indicates that the totally geodesic solutions are not stable. Also, notice that the growth rate increases with the order, which indicates that the PCTME is ill-conditioned, as is also the case for the L^2–TME. Again, our investigation indicates that the dynamics of the PCTME is similar to that of the L^2–TME. We plan to carry out a more thorough investigation of the spectral behaviour, by using both analytical and numerical techniques.

7 Conclusions

In this paper we have studied a geodesic equation on the manifold of planar conformal embeddings. We showed that that the equations have a totally geodesic submanifold corresponding to linear conformal maps. We also showed that the submanifold of affine conformal maps is not totally geodesic. Numerical experiments indicates that the dynamic behaviour of the equation is similar to that of the L^2–TME.

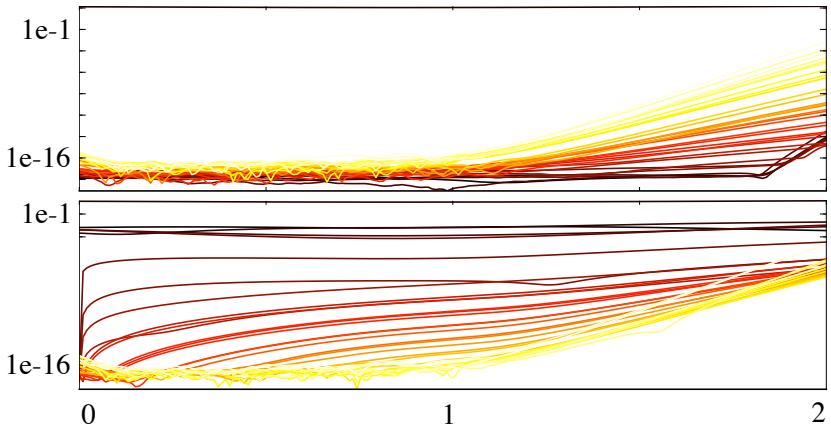

Fig. 3. Time evolution of the absolute values of $\boldsymbol{p_c}$ for a totally geodesic solution computed with the numerical method. *(Top):* without perturbation, *(bottom):* a random perturbation of size $\sim 10^{-4}$ of initial data for the first five coefficients.

In future work we will study the spectral behaviour more thoroughly. Also, as an approach for obtaining more well behaved dynamics, we will consider other metrics, in particular H^1_α. We will also look into more advanced numerical techniques for solving the equations.

References

1. Younes, L.: Shapes and Diffeomorphisms. Applied Mathematical Sciences. Springer-Verlag (2010)
2. Thompson, D.: On Growth and Form. Cambridge University Press (1942)
3. Wallace, A.: D'Arcy Thompson and the theory of transformations. Nature Reviews Genetics **7** (2006) 401–406
4. Camassa, R., Holm, D.D.: An integrable shallow water equation with peaked solitons. Phys. Rev. Lett. **71** (1993) 1661–1664
5. Hamilton, R.S.: The inverse function theorem of Nash and Moser. Bull. Amer. Math. Soc. (N.S.) **7** (1982) 65–222
6. Sharon, E., Mumford, D.: 2d-shape analysis using conformal mapping. Int. J. Comput. Vis. **70** (2006) 55–75 10.1007/s11263-006-6121-z.
7. Marsland, S., McLachlan, R.I., Modin, K., Perlmutter, M.: Reduced geodesic equation for planar conformal embeddings. In preparation (2011)
8. Modin, K., Perlmutter, M., Marsland, S., McLachlan, R.I.: On Euler-Arnold equations and totally geodesic subgroups. J. Geom. Phys. **61** (2011) 1446–1461
9. Holm, D.D., Marsden, J.E.: Momentum maps and measure-valued solutions (peakons, filaments, and sheets) for the EPDiff equation. In: The breadth of symplectic and Poisson geometry. Volume 232 of Progr. Math. Birkhäuser Boston, Boston, MA (2005) 203–235
10. McLachlan, R.I., Marsland, S.: N-particle dynamics of the Euler equations for planar diffeomorphisms. Dyn. Syst. **22** (2007) 269–290
11. Chertock, A., Toit, P., Marsden, J.E.: Integration of the EPDiff equation by particle methods. (2009)
12. Duren, P., Schuster, A.: Bergman Spaces. Volume 100 of Mathematical Surveys and Monographs. American Mathematical Society, Providence, RI (2004)